

A study of the properties of the $\text{YBa}_2\text{Cu}_3\text{O}_{7-\delta}$ high temperature superconductor

K. NAUKKARINEN, K. ARLAUSKAS

Electron Physics Laboratory, Helsinki University of Technology SF-02150 Espoo, Finland

L. GRÖNBERG

Semiconductor Laboratory, Technical Research Centre of Finland, SF-02150 Espoo, Finland

R. LAIHO, J. VANHATALO

Wihuri Physical Laboratory, University of Turku, SF-20500 Turku, Finland

High temperature, $T_c > 90$ K, superconductivity in $\text{YBa}_2\text{Cu}_3\text{O}_{7-\delta}$ samples was observed from resistivity and magnetic susceptibility measurements. The zero-field-cooled susceptibility of the material was 60 to 100% of the ideal diamagnetic value depending on sample preparation. Structure identification by X-ray diffraction at both 293 and 89 K exhibited the same orthorhombic structure. Scanning tunnelling microscope investigations of the sample surface revealed steep step structure with $10 \times 10 \text{ nm}^2$ size crystallites and 5 to 100 nm high terraces. Temperature cycling between 77 and 293 K sometimes led to the appearance of white barium lumps on the surface and in the bulk of the sample causing the transition to the low resistance state at 90 K to disappear.

1. Introduction

Superconductivity in $\text{La}_{2-x}\text{Ba}_x\text{CuO}_4$ near 30 K was discovered by Bednorz and Müller [1, 2]. These results and the following development, especially the attainment of superconductivity at around 90 K by Wu *et al.* [3] and the isolation of the $\text{YBa}_2\text{Cu}_3\text{O}_{7-\delta}$ phase [4] stimulated an increasing number of experimental and theoretical investigations. It is suggested that the critical temperature depends not only on the chemical composition of the superconductive material [5-8], but is also sensitive to sample preparation conditions [8-10], such as annealing temperature [11], oxygen pressure [10] and rate of removal from the furnace after the final annealing [9], which influence stoichiometry, cell symmetry, Cu(3)/Cu(2), Cu/O ratios and oxygen vacancies [10-12] in $\text{YBa}_2\text{Cu}_3\text{O}_{7-\delta}$ compounds. The oxygen loss can significantly change the valence state of copper, and thus influence T_c . Material prepared by the usual sintering method is polycrystalline with strained and bent intergranular bonds, which can have an effect on the low resistance state of the superconductor. In the present paper we report on superconductivity, characterization and ageing of $\text{YBa}_2\text{Cu}_3\text{O}_{7-\delta}$.

2. Results

2.1. Material preparation

$\text{YBa}_2\text{Cu}_3\text{O}_{7-\delta}$ was prepared by mixing BaCO_3 , Y_2O_3 and CuO powders [4]. After heating for about 20 h at 950°C in air, the material was ground, mixed and pressed into pellets. The pellets were sintered at 950°C in flowing oxygen for about 20 h and then slowly cooled down to room temperature. Grinding, mixing,

pressing into pellets and sintering were usually repeated several times.

2.2. Resistivity

Bar-shaped samples (cross section $\sim 10^{-2} \text{ cm}^2$) were cut from the pellets for electrical resistivity measurements. Contacts were made using silver paint, although these contacts had a relatively high contact resistance (sample + contact resistance $\sim 3 \Omega$, while estimated sample resistance $\sim 0.3 \Omega$). For high current-density measurements H-shaped samples (cross-section $\sim 2 \times 10^{-3} \text{ cm}^2$) were used in order to enlarge the contact area at the current probes. Four probe resistivity measurements using both a.c. and d.c. techniques were made. In Fig. 1 are the results from a typical sample. As shown in the figure the sample

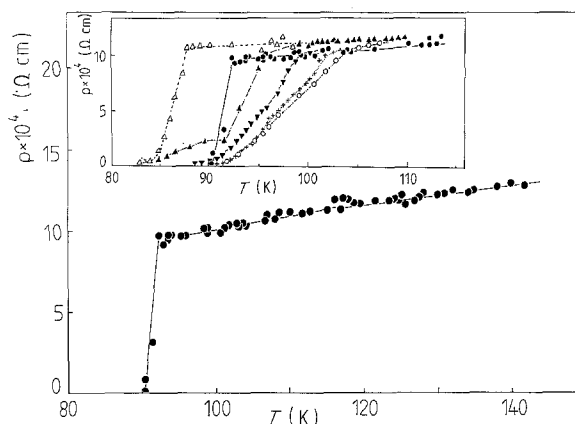


Figure 1 Resistivity as a function of temperature in $\text{YBa}_2\text{Cu}_3\text{O}_{7-\delta}$. (+ $I_{dc} = 1 \text{ mA}$, O $I_{dc} = 10 \text{ mA}$, Δ $I_{dc} = 100 \text{ mA}$, \bullet $I_{ac} = 29 \mu\text{A}$, \blacktriangle $I_{ac} = 290 \mu\text{A}$, \blacktriangledown $I_{ac} = 1 \text{ mA}$).

TABLE 1 Transition temperatures of the resistivity

Current (A)	Low resistance T_c (K)	Midpoint T_c (K)	Onset of transition T_c (K)	Transition width ΔT_c (K)
I_{ac} 2.9×10^{-5}	90.4	91.5	92.5	2.1
1×10^{-4}	90	92.8	95.7	5.7
2.9×10^{-4}	84	93.3	96.7	8.3
1×10^{-3}	89	95.5	99	10
I_{dc} 2×10^{-3}	87.5	93.8	96.3	8.8
1×10^{-2}	91	97	103.2	12.2
1×10^{-1}	83.7	86.3	87.7	8

is in the low resistance state at 90 K. The resistivity at liquid nitrogen temperature was lower than the sensitivity of about $1 \mu\Omega\text{cm}$ of the measurement system. For both a.c. and d.c. measurements the transition width ΔT_c increased with current (Table I, and insert in Fig. 1). However, for a d.c. current density of 10 A cm^{-2} the low resistance point T_c was shifted from 91 to 83 K. The effect can be caused by contact heating or the sample having regions with non-zero resistivity below T_c , possibly the intergranular regions [13, 14]. The transition width for the best samples at low current densities (less than 0.1 A cm^{-2}) was about 2 K. The critical current with the sample immersed in liquid nitrogen was higher than 40 A cm^{-2} . Room temperature resistivities were about $3.1 \text{ m}\Omega\text{cm}$ and about $1.1 \text{ m}\Omega\text{cm}$ at the onset of the transition.

2.3. Magnetization and susceptibility

Magnetization and susceptibility measurements were made with an r.f.-SQUID magnetometer by using cylindrical samples having a typical volume of 0.02 cm^3 (demagnetization factors 0.15). At low temperature the zero-field-cooled susceptibility was between 60 and 100% of the ideal diamagnetic value depending on the sample preparation (Fig. 2). Sample 2 (circles) was pressed into pellets at higher pressure than sample 1 (triangles). For both samples the susceptibility changes from paramagnetic to diamagnetic at 90 K. The paramagnetic susceptibility just above the transition temperature corresponds to a value of $2.4 \times 10^{-4} \text{ emu cm}^{-3}$. The magnetization of sample 1 rises linearly with a slope of $-1/4$ up to

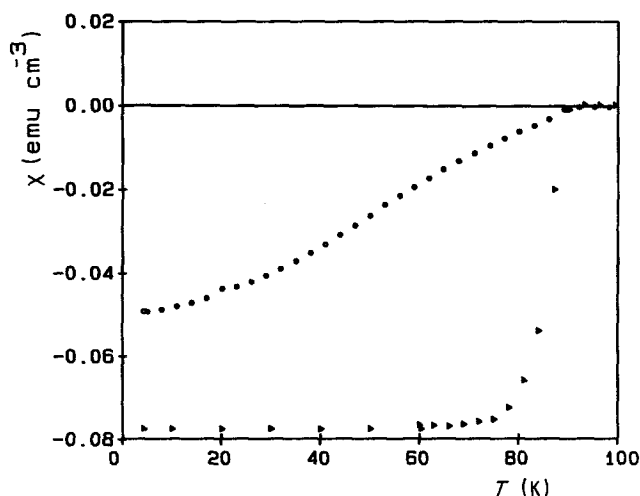


Figure 2 Zero-field-cooled susceptibility plotted against temperature for sample 1 (\blacktriangle) and sample 2 (\circ). The measuring field was $1 \times 10^{-3} \text{ T}$.

about 0.04 T where the flux starts to penetrate the sample (Fig. 3, triangles). In the case of sample 2 (circles) the initial slope is much smaller indicating smaller superconducting volume fraction in this sample.

In the magnetization measurements time dependent effects, probably due to flux creep, were observed. As typical to irreversible type II superconductors, the time decay of magnetization was approximately logarithmic.

2.4. X-ray diffraction

To investigate possible structural transformation of the crystal, causing the high T_c superconductive state [15–17], X-ray diffraction patterns of powdered samples and thin pellets were taken at 293 and 89 K (Figs 4 and 5). These patterns exhibited the same orthorhombic structure for both temperatures. In addition to sharp lines, a definite broad ring in the transmission Laue picture was seen at a small angle around the position of the 003 and 010 reflections (Fig. 5). Such rings are typical for local changes in the electron density, caused by amorphous regions between the grains or microtwins inside the grains or the presence of more than one phase in the sample. According to Fig. 4 the $\text{YBa}_2\text{Cu}_3\text{O}_{7-\delta}$ phase is pure in our samples thus eliminating the last assumption.

2.5. Scanning tunnelling microscopy

Microstructural investigations made with a scanning tunnelling microscope revealed a great number of submicrometre grains with a broad distribution in

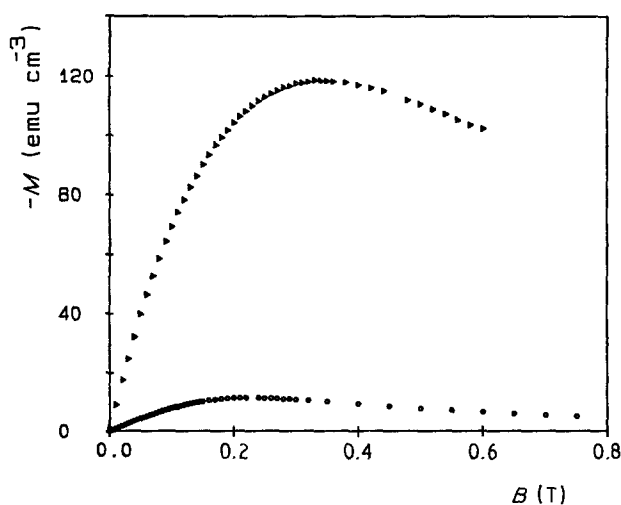


Figure 3 Magnetization of sample 1 (\blacktriangle) and sample 2 (\circ) at 4.2 K as a function of external magnetic field.

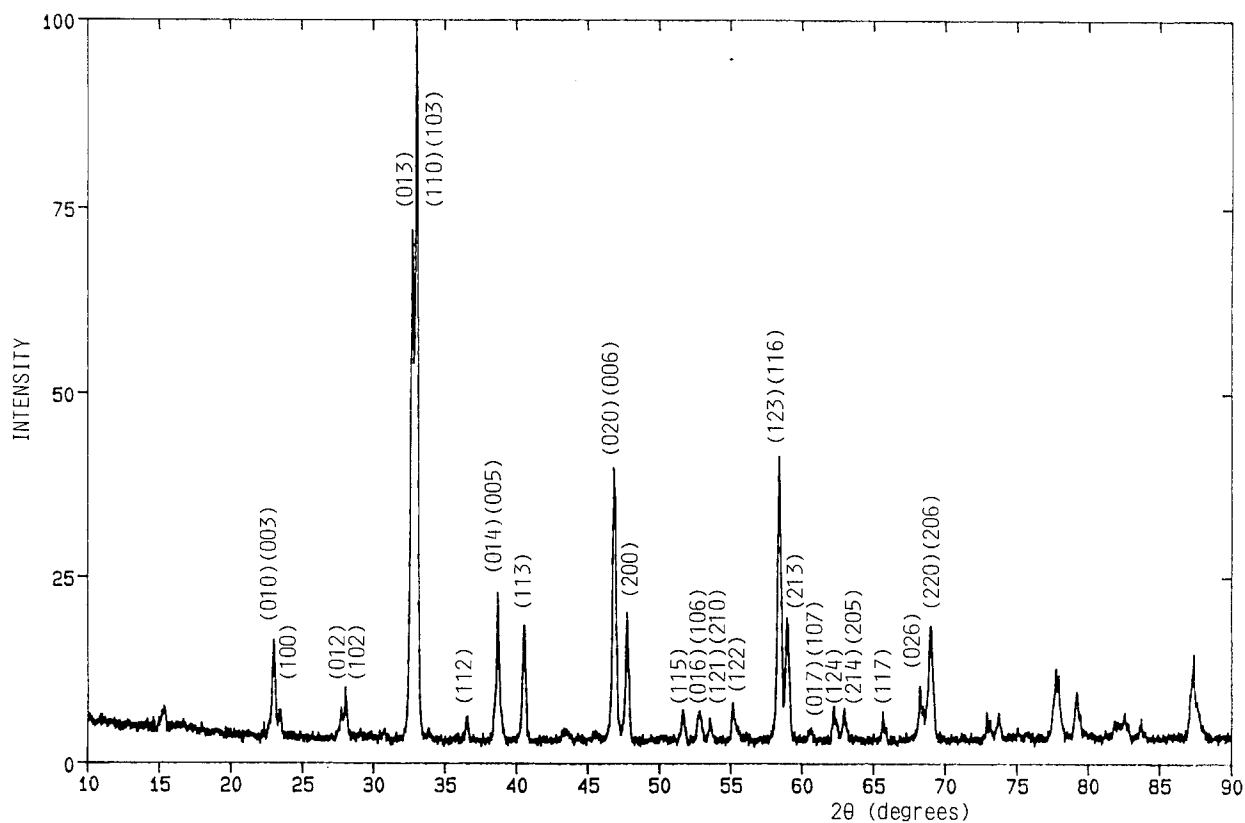


Figure 4 X-ray diffraction pattern of $\text{YBa}_2\text{Cu}_3\text{O}_{7-\delta}$.

size and orientation. Typical surface topologies included fairly smooth plateau of more than $10 \times 10 \text{ nm}^2$ in size, well defined step structures with a height from 5 to over 100 nm and arrays of 10 to 50 nm wide patterns of clusters (Fig. 6a) separated by deep narrow valleys. In Fig. 6b a complex surface corrugation is shown including a pattern of small grains, similar to those in Fig. 6a, in its left hand corner.

Similar structures were observed both from the surface formed when the pellet was pressed against its container and from the surface formed by breaking a sample pellet. The great number of surface irregularities having dimensions of the order of a few unit cell lengths suggests corresponding fluctuations in the local elastic and electronic properties of our samples.

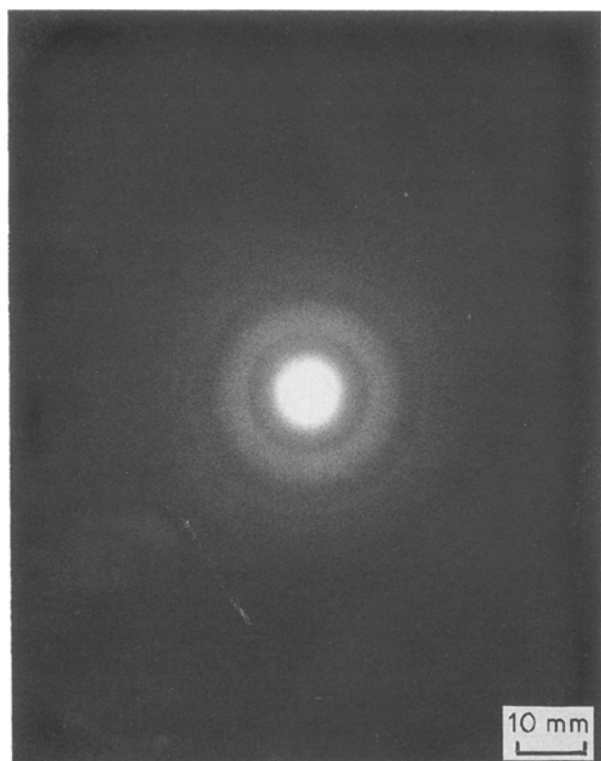


Figure 5 Transmission Laue X-ray diffraction pattern of $\text{YBa}_2\text{Cu}_3\text{O}_{7-\delta}$ at 89 K. The film was placed 6 cm behind the crystal. CuK_α radiation was used.

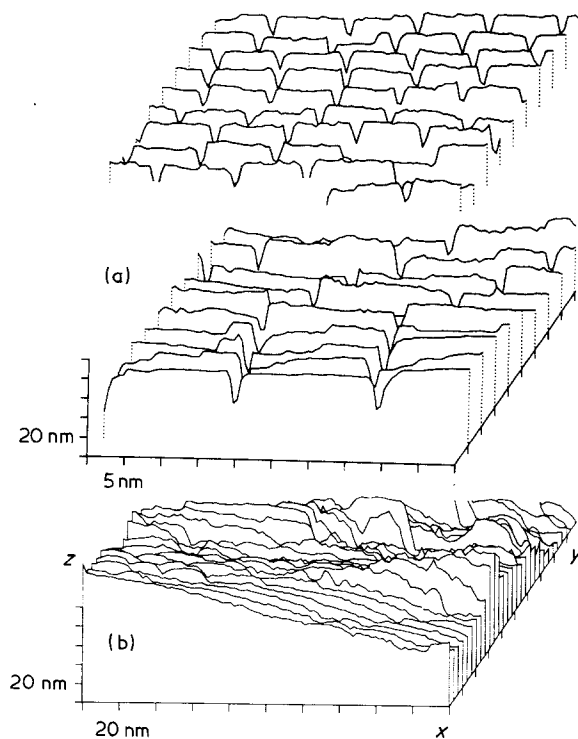


Figure 6 Surface topologies of $\text{YBa}_2\text{Cu}_3\text{O}_{7-\delta}$ observed by a scanning tunnelling microscope. In (a) is shown regular arrays of small grains separated by valleys and in (b) a complex surface corrugation involving a pattern of clusters in its left hand corner. Pictures (a) and (b) were obtained from different sample pellets at $T = 300 \text{ K}$.

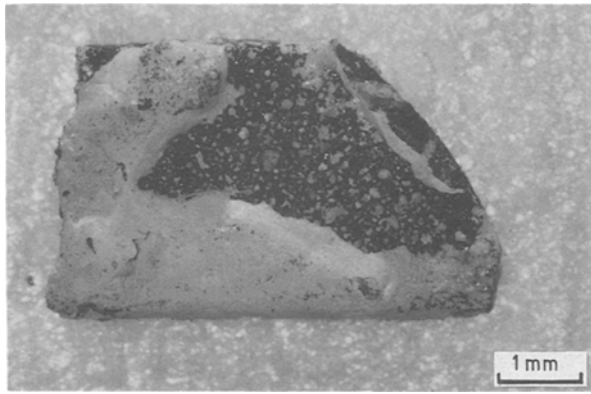


Figure 7 $\text{YBa}_2\text{Cu}_3\text{O}_{7-\delta}$ sample after it has been dipped into liquid nitrogen and heated to room temperature several times.

This agrees with the observation of a broad ring in the Laue picture.

Assuming that the superconducting grains are coupled together by Josephson tunnelling or proximity effect a superconductor is predicted to show spin-glass like properties [18]. Such situations may occur in our samples in the case that the plate-like grains, as shown in Fig. 6, carry supercurrent loops which are weakly coupled either through the valleys between the grains or inductively from grain to grain. The supercurrent loops correspond to weakly interacting magnetic moments in an ordinary spin-glass and lead to spin-glass like properties of the superconductor.

2.6. Stability

The sample resistivity was found to have increased after cooling it down to liquid nitrogen temperature and heating it up to room temperature during the measurements. In some cases white lumps of barium (as determined by Auger spectroscopy) were found on the surface and in the bulk of the sample. The appearance of barium led to a destructive increase of the resistivity. However, these samples still levitated at liquid nitrogen temperatures in a magnetic field, indicating that parts of the sample were still superconductive. The appearance of barium was also detected in samples without contacts that were dipped into liquid nitrogen and heated to room temperature several times (Fig. 7).

3. Conclusions

In conclusion, (i) we observed a transition to the superconductive state in $\text{YBa}_2\text{Cu}_3\text{O}_{7-\delta}$ at 90 K, (ii) the transition width increases with current, (iii) at low temperatures the susceptibility of the material was 60 to 100% of the ideal diamagnetic value, (iv) X-ray diffraction patterns taken at 293 and 89 K exhibited the same orthorhombic crystal structure, (v) X-ray

diffraction and scanning tunnelling microscope investigations showed that the material consists of crystallites with possible amorphous intergrain regions, and (vi) temperature cycling lead to outdiffusion of barium, which destroys the low resistance state of the sample and decreases the volume of the superconductive material of the sample.

References

1. J. G. BEDNORZ and K. A. MULLER, *Z. Phys. B* **64** (1986) 189.
2. J. G. BEDNORZ, M. TAKASHIGE and K. A. MULLER, *Europhys. Lett.* **3** (1987) 379.
3. M. K. WU, J. R. ASHBURN, C. J. THORNG, P. H. HOR, R. L. MENG, L. GAO, Z. J. HUANG, Y. Q. WANG and C. W. CHU, *Phys. Rev. Lett.* **58** (1987) 908.
4. R. J. CAVA, B. BATLOGG, R. B. VAN DOVER, D. W. MURPHY, S. SUNSHINE, T. SIEGRIST, J. P. REMEIK, E. A. RIETMAN, S. ZAHURAK and G. P. ESPINOSA, *ibid.* **58** (1987) 1676.
5. P. H. HOR, R. L. MENG, Y. Q. WANG, L. GAO, Z. J. HUANG, J. BECHTOLD, K. FORESTER and C. W. CHU, *ibid.* **58** (1987) 1891.
6. S. HOSOYA, S. SHAMOTO, M. ONODA and M. SATO, *Jpn J. Appl. Phys.* **26** (1987) L325.
7. *Idem.*, *ibid.* **26** (1987) L456.
8. Y. MAENO, M. KATO and T. FUJITA, *ibid.* **26** (1987) L329.
9. P. M. GRANT, R. B. BEYERS, E. M. ENGLER, G. LIM, S. S. P. PARKIN, M. L. RAMIREZ, V. Y. LEE, A. NAZZAL, J. E. VAZQUEZ and R. J. SAVOY, *Phys. Rev. B* **35** (1987) 7242.
10. P. STROEBEL, J. J. CAPPONI, C. CHAILLOUT, M. MAREZIO and J. L. THOLENCE, *Nature* **327** (1987) 306.
11. A. OURMARD, J. A. RETSCHLER, J. C. H. SPENCE, M. O'KEEFFE, R. J. GRAHAM, D. W. JOHNSON Jr and W. W. RHODES, *ibid.* **327** (1987) 308.
12. W. I. F. DAVID, W. T. A. HARRISON, J. M. F. GUNN, O. MOZE, A. K. SOPER, P. DAY, J. D. JORGENSEN, D. G. HINKS, M. A. BENO, L. SODERHOLM, D. W. CAPONE II, I. K. SCHULLER, C. U. SEGRE, K. ZHANG and J. D. GRACE, *ibid.* **327** (1987) 310.
13. S. KOGOSHIMA, S. HIKAMI, Y. NOGAMI, T. HIRAI and K. KUBO, *Jpn J. Appl. Phys.* **26** (1987) L318.
14. X. CAI, R. JOYNT and D. C. LARBALESTIER, *Phys. Rev. Lett.* **58** (1987) 2798.
15. J. YU, A. J. FREEMAN and J.-H. XU, *ibid.* **58** (1987) 1035.
16. L. F. MATTHEISS, *ibid.* **58** (1987) 1028.
17. J. D. JORGENSEN, H. B. SCHUTTLER, D. G. HINKS, D. W. CAPONE II, K. ZHANG, M. B. BRODSKY and D. J. SCALAPINO, *ibid.* **58** (1987) 1024.
18. C. EBNER and D. STROUD, *Phys. Rev. B* **31** 165 (1985).

Received 2 March
and accepted 18 July 1988